Journal of Electronic Materials, Vol. 19, No. 3, 1990

JNC.1.T1

Reaction Pathways and Sources of OH Groups in Low Temperature Remote PECVD Silicon Dioxide Thin Films

J. A. THEIL, D. V. TSU and G. LUCOVSKY

Departments of Physics, and Materials Science and Engineering
North Carolina State University, Raleigh, NC, 27695-8202

Silicon oxides deposited by remote plasma-enhanced chemical-vapor deposition (Remote PECVD) can be grown under conditions which produce hydrogen-free SiO_2, and under conditions which promote the incorporation of bonded-hydrogen in either SiH or SiOH groups, but generally not in both. In this paper, we investigate the relationship between the deposition conditions leading to OH incorporation, and other post-deposition pathway(s) by which OH can also be incorporated. Two ways by which OH can be incorporated into the oxides are by: (i) *intrinsic* pathways which are associated with the heterogeneous chemical reactions responsible for film growth; and (ii) *extrinsic* pathways which refer to incorporation after film deposition stops. The results of our experiments to date show no evidence to support the intrinsic process; all of the infrared (ir) detectable OH is shown to derive from post-deposition or extrinsic sources. We have found two distinct post-deposition sources, one from the deposition chamber ambient during cool-down and one from atmospheric moisture. Each of these sources has a particular spectroscopic signature. We show that OH incorporated from atmospheric moisture occurs as spatially correlated near-neighbor Si-OH groups, whereas OH groups incorporated in the deposition chamber ambient are randomly distributed in the SiO_2 host material.

Key words: Chemical vapor deposition, plasma enhanced chemical vapor deposition, dielectric thin films, OH in silica, SiO_2, silicon dioxide, SiO_2 ir spectroscopy

I. INTRODUCTION

There is considerable interest in producing stable, electronic-quality dielectrics, such as SiO_2, at low temperatures. Plasma- and photo-enhanced chemical-vapor deposition are attractive alternatives for this application due to the lower substrate temperatures they require when compared with the high temperature pyrolytic CVD processes. However, one of the chief concerns is chemically bonded hydrogen in SiO_2 films produced at low temperatures. For example, it has been shown that films deposited by conventional direct plasma-enhanced chemical-vapor deposition (PECVD) generally contain between 5 and 10 at. % *unintentionally* incorporated hydrogen bonded in both Si-H and Si-OH groups,[1,2] but that the concentration of bonded hydrogen in SiO_2 films grown by Remote PECVD can be reduced to levels below the range of infrared (ir) detection, less than about 1 at. %. In addition, deposition conditions and specific reaction pathways have been identified by which controlled amounts of SiH can be *intentionally* incorporated into the Remote PECVD SiO_2 films.[3,4,5] We have previously identified process conditions under which OH groups can also be *intentionally* incorporated into Remote PECVD SiO_2 thin films, and this paper identifies some of the specific reaction pathways involved in these processes.[5]

All PECVD techniques involve the plasma excitation of at least some of the gaseous species in order to produce the chemically reactive species that promote low temperature thin film deposition. In Direct PECVD the substrate and all of the gases in the deposition chamber are exposed to the plasma. This condition generally leads to many simultaneous, or *parallel* deposition reaction pathways, thereby making it difficult, if not impossible, to control both the stoichiometry (in the context of the Si/O ratio) and chemical purity of deposited materials.[1] There is one notable exception to this generalization: this is the Batey-Tierney process for deposition of SiO_2 by a Direct PECVD process in which extremely high dilution of the process gases limits precursor formation and reactions pathways, and thereby leads to the formation of stoichiometric, hydrogen-free films.[6]

The Remote PECVD process affords greater control over the thin film chemistry when compared to conventional Direct PECVD, by restricting plasma excitation to a subset of the process gases, and thereby reducing the multiplicity of reaction pathways. The physical arrangement of the chamber is such that the process flow is *sequential or serial,* rather than *parallel* as in Direct PECVD. A subset of the process gases are excited in a tube that is located outside of the deposition chamber. Plasma-excited species then flow out of the plasma-generation region into the deposition chamber and mix with the remaining unexcited process gases. The excited species extracted from the plasma excitation tube and the unexcited species injected downstream react heterogeneously at the substrate to produce the desired thin film.[7,8] For the deposition of SiO_2,

(Received July 26, 1989)

0361-5235/1990/1401-209$5.00©90 AIME

Si_3N_4, and SiO_xN_y alloys, process gases, such as SiH_4, and Si_2H_6, etc., are always injected downstream and are never directly exposed to the plasma. This prevents gas-phase activation of the silanes and thereby eliminates deposition reaction pathways that can promote either non-stoichiometry in the Si:O and/or Si:N ratios, or the incorporation of bonded hydrogen in SiH configurations.

The reaction pathways for the deposition of hydrogenated amorphous silicon (a-Si:H) and SiO_2 have been studied primarily by mass spectrometry (MS).[4] We have identified two *balanced* reaction equations for the deposition of the SiO_2 films, and one for a-Si:H:

$$(He + 2O_2)^* + SiH_4 \rightarrow SiO_2 + 2H_2O \quad (1)$$

$$(He + O_2)^* + SiH_4 \rightarrow SiO_2 + 2H_2 \quad (2)$$

$$(He)^* + SiH_4 \rightarrow \text{a-Si:H} + 2H_2 \quad (3)$$

where the * refers to the plasma excited gases.[4] The amorphous silicon reaction proceeds only when electrons and ions are extracted from the plasma generation region, *i.e.*, only when the plasma afterglow extends into the deposition chamber, thereby exciting, but not fragmenting, the silane.[9] The oxides on the other hand, do not require that silane be excited in the plasma afterglow. We briefly describe in the following section how silane is excited in one case, but not in the other. For the oxides, either O_2 or N_2O may be used as the oxygen source. We have found that O_2 is the major by-product of the plasma excitation of N_2O, and therefore the deposition reactions are effectively the same as reactions (1) and (2).[10] In general, suboxides, *i.e.*, oxides containing Si-Si and/or Si-H bonding groups, are produced when the following two conditions are met: (i) the O_2/SiH_4 ratio is <1; and (ii) silane is exposed to the plasma afterglow.[5] It is not simply a lack of O_2 which leads to suboxides, since SiO_2 can be deposited for O_2/SiH_4 ratios as small as 0.1 as long as the silane reactant is not plasma activated. Suboxides are generally produced by the codeposition of SiO_2 and a-Si:H, *i.e.*, by the reactions (2) and (3) occurring simultaneously.[5] For this study, the silane was therefore not plasma activated to produce the oxide thin films.

The MS studies we have performed show that for O_2 concentrations in He greater than about 2%, reaction (1) dominates, whereas for concentrations below about 2%, reaction (2) dominates. We have generally found that high O_2 concentrations (>2% in He), low temperatures (<250° C) and high deposition rates (>1Å/s) result in ir-observable OH incorporation; higher temperatures (>250° C), lower O_2 flow rates and lower deposition rates (<0.2Å/s), serve to minimize, or to eliminate the OH incorporation.[3] These films can however, under prolonged exposure to atmospheric moisture (on a time scale of months or years), display measurable ir absorbance in the OH band.

In this paper, we have examined films which were grown with the intention of including bonded OH to study the mechanisms by which OH groups can be incorporated into the SiO_2 films. In particular, two different pathways are possible by which OH can be incorporated into the SiO_2 films: (i) intrinsic pathways, and (ii) extrinsic pathways. The intrinsic pathways are intimately associated with the heterogeneous chemical reactions responsible for film growth.[12] Extrinsic pathways refer to incorporation mechanisms after film growth has occured. An earlier study by Pliskin[11] has shown that OH groups can be incorporated in CVD oxides by extrinsic processes, *e.g.*, when the films have been exposed to atmospheric water vapor. A primary goal of this paper is to determine whether the differences in OH incorporation under the conditions discussed above, result from intrinsic or extrinsic processes. With the use of a-Si:H diffusion barriers, we confirm in this report that the extrinsic process accounts for all ir observable OH in Remote PECVD oxides, particularly those deposited under the conditions of high oxygen flow and high deposition rates. Under the conditions we have investigated, no evidence is found to support an intrinsic OH incorporation process.

II. EXPERIMENTAL APPARATUS AND FILM DEPOSITION

The deposition chamber for these experiments is constructed of 5.1 cm outer diameter × 46 cm long stainless steel tube (see Fig. 1).[4] Plasmas are generated by coupling rf excitation (~10–20 W at 13.56 MHz) into a plasma tube (32 mm outer diameter vitreous silica tubing) located at one end of the deposition chamber. The deposition chamber consists of the plasma bias assembly, two gas dispersal rings, and five analyzing stations. The plasma bias assembly is located immediately *downstream* from the plasma tube and consists of four Al plates and a #10 stainless steel screen grid, each of which is electrically isolated from the chamber. The Al plates are in a box-like configuration oriented coaxially with the chamber, and the grid caps located at the downstream end of the box. One analyzing station is between the first gas dispersal ring and the bias assembly, the other gas ring is located 10 in. downstream from the first ring. There are three analysis stations between the gas rings with one station beyond the second gas ring. Each station consists of three ports, one for mass spectrometer sampling, and two for optical studies, *e.g.*, by optical emission spectroscopy (OES). The sample is mounted on a 2.5 cm o.d. copper block with a 250 W lamp and thermocouple imbedded in it. The block is mounted on the end of a polished 91 cm long SS tubular linear feed-through and is sealed by a differentially pumped mechanism. The process pressure is measured by an MKS capacitance manometer which controls a downstream throttle valve. A 400 l/s turbomolecular pump in the MS chamber also services the deposition chamber and achieves a base pressure of $<2 \times 10^{-7}$ Torr in the deposition chamber. The *in-*

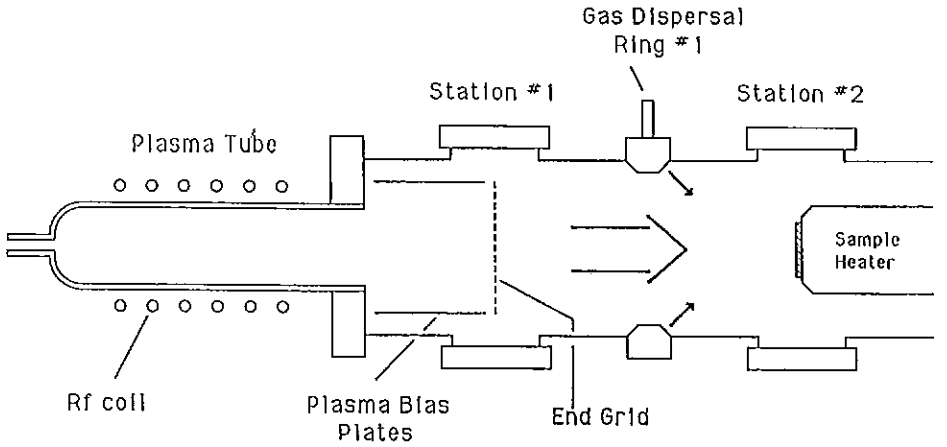

Fig. 1 — Diagram of The Remote PECVD Deposition/Analysis Chamber.

situ analytical equipment consists of an Extrel C-50 quadrapole mass spectrometer (MS) and a Tracor Northern TN-6500 optical multichannel analyzer.

The grid is normally biased in one of two states, either tied to the ground potential of the chamber, or floating and thereby electrically isolated from the rest of the chamber; the four Al plates are always held in the floating state. In the grid grounded state, the plasma after-glow (consisting of electrons and ions) can extend beyond the grid and into the chamber, while in the floating state, the plasma is contained behind the grid and no charged particles are injected into the deposition region. For the a-Si:H *capping layers* we have used in these experiments, the grid is grounded in order to provide excitation of the silane; whereas for the oxide depositions, it is floating to prevent excitation of the silane, and the consequent formation of hydrogenated suboxides.

To produce the SiO_2 films, a mixture of 10–20% O_2 or N_2O in He flowing at a total flow rate of 100 standard cm^3/min (sccm), is rf excited (8 to 17 W), with the chamber pressure maintained at 300 m Torr during deposition. A mixture of 10% SiH_4 in Ar is injected through the first gas dispersal ring at a rate of 5 to 10 sccm, and the SiH_4 is not directly in contact with the plasma after-glow since the grid is in its floating bias mode. The substrate is positioned at the first station downstream from the first gas ring. The substrate, ({100} *n*-type Si, 10–70 Ω-cm), is typically heated to a temperature (T_S) of 100 to 250° C. To produce the a-Si:H cap the following operations are performed sequentially: the oxygen source is switched off, the rf power is turned up to 32 W, and the bias state of the grid is switched to the grounded mode. Caps of between 800 and 900Å were deposited.

A series of experiments were performed to explore the formation of Si-OH groups. To accomplish this, a-Si:H diffusion barriers were deposited after the deposition of the SiO_2 films to prevent post-deposition OH formation that could result from reactions with ambient water. We have performed the following experiments, (see Table I for a summary of the deposition conditions). The following conditions were maintained to deposit the a-Si:H diffusion barrier: T_S 200° C, He flow 100 sccm, 10% SiH_4 + Ar flow 10 sccm, rf power 31 W, the grid was grounded to the chamber potential. First, a series of SiO_2 films were deposited and capped immediately after deposition to eliminate any post-deposition incorporation processes, (namely from the chamber during cool-down, or outside of the chamber in the laboratory ambient, [approximately 50% RH and 75° F are typical of North Carolina State University physics laboratories in the spring and summer months]). Next, a series of SiO_2 films were capped, but only after permitting exposure of the oxide layer to the chamber ambient for roughly 30 min at 0.3 Torr. These experiments were performed to determine whether OH formation associated with wall contamination, etc., can occur during sample cool-down in the deposition chamber. Finally, SiO_2 films were deposited without any capping to determine the effects of exposure to *moist* laboratory air, and different processing steps on SiOH incorporation via intrinsic mechanisms related to the deposition reaction process pathways.

Table I. Summary of Deposition Conditions for OH Incorporation Source Experiments.

Sample	T_S (°C)	rf Pwr (W)	He flow (sccm)	O flow (sccm)	10% SiH4 + Ar flow (sccm)	Dep. Time (min)	Capping Procedure
AOY10	200	12	80	N_2O 20	10	15	Immediate
AOX92	200	16	90	O_2 10	5	15	Immediate
AOX94	200	17	90	O_2 10	5	15	Held @ 200° C
AOY07	200	12	80	O_2 20	10	20	Cooled to 81° C
AOX89	250	18	90	O_2 10	5	21	None

III. EXPERIMENTAL RESULTS: IR STUDIES

The spectra for the two films deposited at 200° C with capping immediately after deposition are shown in Fig. 2. The "distorted" baselines in these spectra are due to interference fringes characteristic of the a-Si:H-SiO_2 composite thin film structure. The absorption band at 635 cm^{-1} is associated with the SiH bending vibration of the a-Si:H cap. Both spectra in Fig. 2 clearly show the three normal vibrational modes of the Si-O-Si group at 1060, 810, and 445 cm^{-1}, corresponding respectively to stretching (s), bending (b), and rocking (r) motions of the oxygen atom relative to its two silicon neighbors. These spectra show *no* ir evidence for OH or OD incorporation (*i.e.*, in the 3300–3700 cm^{-1} region), and demonstrate that even under the deposition conditions of high oxygen concentration in He (10 to 20% O_2 or N_2O in He) used to produce these films, it is possible to produce SiO_2 films by Remote PECVD containing no OH. In other words, an intrinsic OH incorporation pathway, that might be associated with the by-product water, is not observed. This then establishes that OH formation does not occurs during these conditions of film deposition.

Figure 3 shows the ir spectra characteristic of two different samples made by delaying the capping procedure. The sample that was held at 200° C during the delay periods, AOX94, does not display any OH feature that can be detected via ir, while the sample that cooled to 81° C, AOY07, does. The absorption band due to the internal O-H stretching vibration, OH(s), for sample AOY07 is asymmetric, with a peak at about 3650 cm^{-1}. Table II shows the peak positions and the full width at half maximum absorbance (FWHM) of the SiO(s) band for these two films in which capping was delayed, but under different conditions. Note that the film held at 81° C prior to capping has a SiO(s) band spectral peak that is higher in wavenumber than the film held at 200° C. This is consistent with the observations made on uncapped films wherein the spectral peak position increases with increasing OH incorporation.

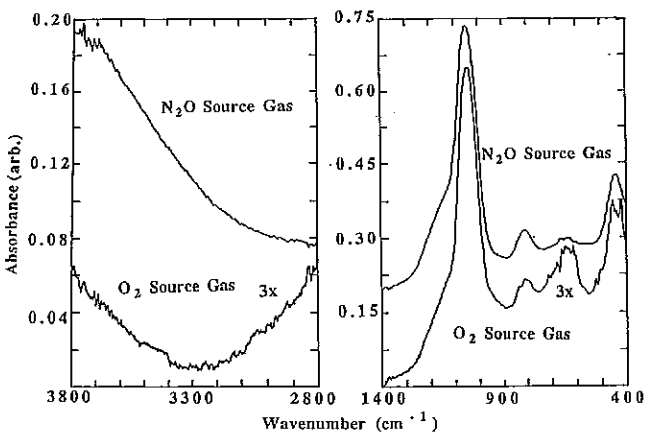

Fig. 2 — Ir spectra of Composite Films with Immediate Capping. a) OH(s) band at 3550 cm^{-1}, b) SiO(s) 1060 cm^{-1}. 445 cm^{-1}. Neither sample (N_2O or O_2 source gas) shows evidence of OH incorporation.

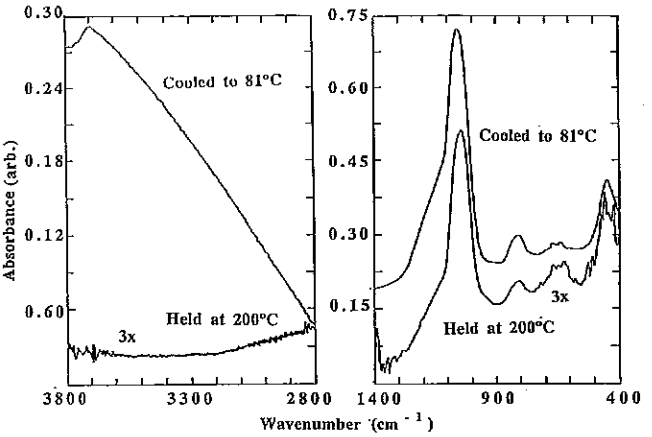

Fig. 3 — Ir spectra of Composite Films with Delayed Capping. a) OH(s) band at 3550 cm^{-1}, b) SiO(s) 1060 cm^{-1}. The sample that was cooled to 81° C shows evidence of OH incorporation, while the sample that was held at 200° C shows no evidence of OH incorporation.

The spectra shown in Fig. 4(a) and (b) are taken from sample AOX89, which has no a-Si:H cap, *immediately* after deposition, and 2, 3 and 5 days after removal from the chamber. Note that these films show evidence for OH groups in the first spectrum in this series giving the time evolution of the Si-OH group. The incorporation of OH groups can lead to changes in the structure of the SiO(s) band, as shown in Fig. 4(a) and 4(b) showing the OH(s) and SiO bands, respectively. With increasing OH incorporation there are three changes in the SiO(s) band: (i) the spectral peak shifts to higher wavenumber, from 1055 to 1064 cm^{-1}, (ii) the band width (FWHM) decreases from 94 to 82 cm^{-1}, and (iii) the absorption in the high wavenumber shoulder increases. In addition, there is the development of a satellite feature at about 925 cm^{-1}. These trends are displayed graphically in Fig. 5.

The OH incorporation in the film is accompanied by the appearance of the OH(s) band centered at approximately 3550 cm^{-1} as shown in Fig. 4. Initially, an *asymmetrically* shaped OH(s) band appears with a peak at about 3650 cm^{-1}. The OH producing this asymmetric feature either developed after film growth but before removal from the chamber, or it developed rapidly after removing the sample from the deposition chamber (the time interval between sample removal and initiation of the ir spectrum is on the order of minutes). But the growth of a second *symmetric* feature, centered at about 3350 cm^{-1}, is evident in the traces labelled 2 days or

Table II. Comparison of Delayed Capped Oxide Films. FWHM is the Abbreviation of the Full Width Half Maximum of the Band.

	Held at 200° C	Cooled to 81° C
SiO(s) Band	1046 cm^{-1}	1060 cm^{-1}
OH(s) Band	Not Detectable	3663 cm^{-1}
SiO(s) FWHM	92.6 cm^{-1}	101.0 cm^{-1}

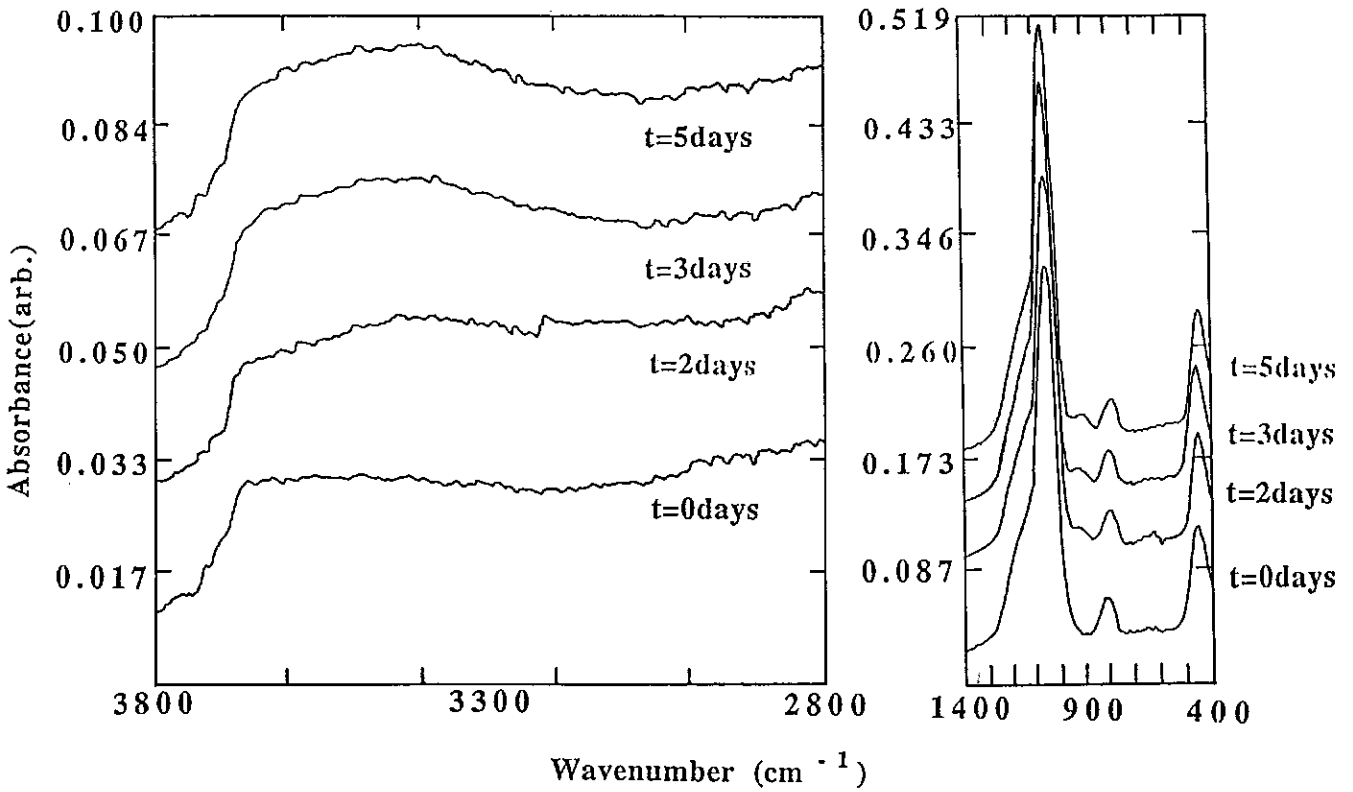

Fig. 4 — Ir Spectra of Uncapped Oxide AOX89 w.r.t. Time. a) OH(s) band at 3550 cm^{-1}, b) SiO(s) 1060 cm^{-1}, SiO(b) 810 cm^{-1}, and SiO(r) 445 cm^{-1}. The 3550 cm^{-1} band shows an asymmetric feature that appears within minutes of deposition, then the appearance of a symmetric feature that appears within days after deposition.

longer; this feature increases in relative intensity on a time scale on the order of days and is clearly associated with exposure to the moist ambient in the laboratory. In other words, an extrinsic OH source is water vapor in the air and the growth of this symmetric band is a spectroscopic hallmark of its incorporation.

Figure 6 includes plots showing changes in the integrated area, and FWHM for the OH(s) band. The FWHM of the band increases from about 372 cm^{-1} to a maximum width of about 425 cm^{-1} after 2 days, then ceases to increase further. It is interesting to note that the SiO(s) FWHM curve behaves in an opposite manner to the OH(s) FWHM curve shown in Fig. 5(b). Along with the growth of the OH(s) band, there is also the formation of a new feature at about 925 cm^{-1}; this is assigned to the SiOH group.[11] This band is not resolved when only an asymmetric OH(s) feature is present, however the region between the SiO(s) and SiO(b) features, between 900 and 1000 cm^{-1}, displays a slightly increased shoulder on the SiO(s) band, when the asymmetrically shaped OH(s) band is present, see Figs. 2(a) and (b), spectra (i).

Finally, two additional experiments were performed to determine the effects of various post-deposition treatments on OH incorporation into the Remote PECVD oxide films, *i.e.*, a boiling study and an annealing study. Sample AOX89 was immersed in boiling deionized (D.I.) H_2O for 30 min, 6 days after it was taken from the chamber. Nine days later, *i.e.*, 15 days after deposition, the ir spectrum of the film was measured again. The film was then flash annealed (FA) in vacuum for two minutes, (at ~700–800° C). Figure 7 contains the ir spectra and Table III shows how different post-deposition treatments changed the position, amplitude, width, and area of the SiO(s) and OH(s) peaks. Surprisingly, after the boiling treatment, the OH(s) band integrated area *decreased,* but 9 days later the film had recovered more than the lost OH, from atmospheric exposure. After the FA, all traces of OH were removed from the film, and the SiO(s) peak position which had increased to 1068 cm^{-1}, decreased to 1063 cm^{-1}. The film was measured again after 90 days and was still found to be OH free.

IV. DISCUSSION

Capped Oxide Experiment Interpretation

The oxides in this study were *intentionally* deposited under conditions *favorable* to the incorporation of OH as confirmed by the ir results of Fig. 4. However, when oxides are produced under the same conditions, but capped immediately after SiO_2 formation by an a-Si:H diffusion barrier, *no* ir measurable OH was found, independent of whether O_2 or N_2O was used in the deposition process. This shows, that within the detection limits of ir spectroscopy, an intrinsic pathway to OH incorporation is not operative, but that an extrinsic post-deposi-

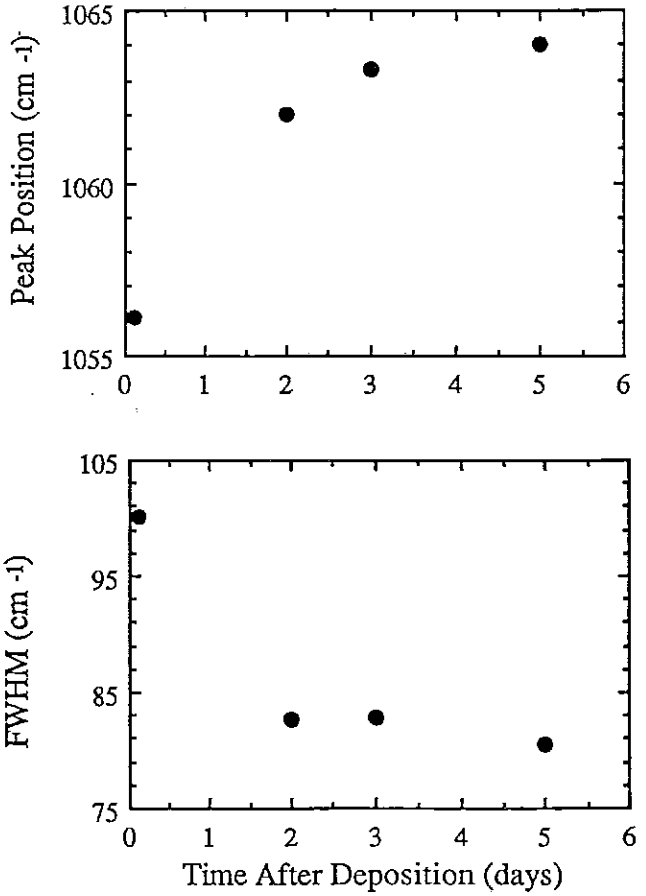

Fig. 5 — Features of the SiO(s) Band for an Uncapped Oxide (AOX89). The plots are the peak position and the FWHM, (Full Width Half Maximum), with respect to time after the oxide was exposed to air.

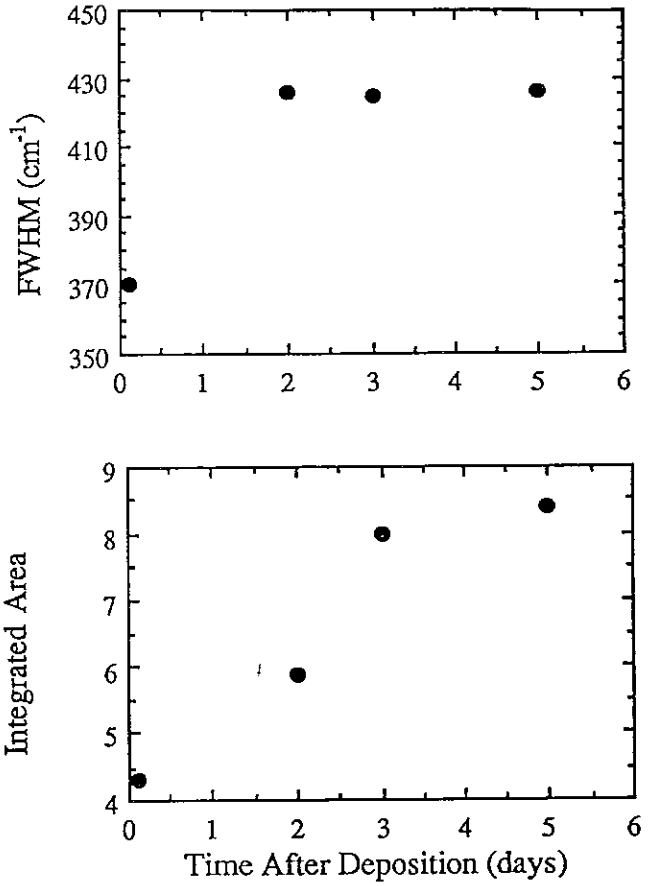

Fig. 6 — Features of the OH(s) Band for an Uncapped Oxide (AOX89). The plots are the FWHM and the integrated area of the band with respect to time after the oxide was exposed to air.

tion pathway is. Moreover, two distinct post-deposition sources have been identified, one is associated with the deposition chamber during sample cooldown, and the other with the absorption by the film of atmospheric moisture.

We have noted above that the incorporation of OH is predominantly an extrinsic process, whether inside or outside of the deposition chamber, but the details of the spectral features associated with the OH groups can be different for these two cases. Specifically, incorporation in the chamber leads to an OH(s) band that is highly asymmetric, whereas incorporation outside leads to a symmetric OH(s) band and the appearance of a discrete spectral SiOH feature at about 925 cm^{-1}. We propose that these spectral differences are associated with different local bonding environments of the Si-OH groups, which in turn reflect aspects of the reaction chemistry which lead to their incorporation. Although it is clear that moisture, H_2O, is the molecular source in the "post-chamber-removal" case, it is not absolutely clear that it is also in the "pre-chamber-removal" case. Either way, as noted above, an asymmetric OH(s) band is formed in the chamber and the time scale for this process is on the order of minutes. The asymmetric shape with its low wavenumber tail, arising from this fast process, leads us to the conclusion that the Si-OH groups are spatially uncorrelated. This band shape is characteristic of a distribution of groups without an average spatial relation. The time scale for the absorption of at-

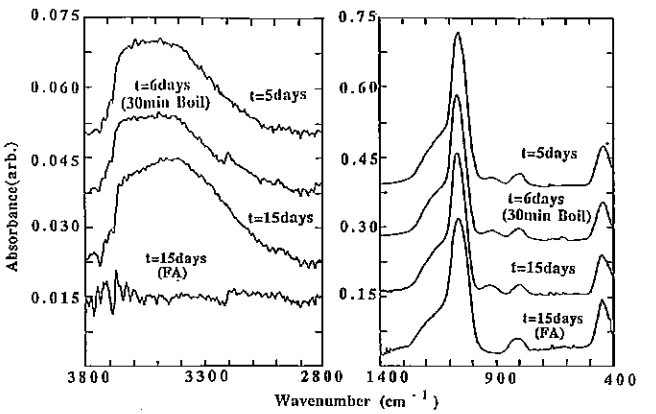

Fig. 7 — Ir Spectra of Uncapped Sample AOX89. a) OH(s) band at 3550 cm^{-1}, b) SiO(s) 1060 cm^{-1}. The spectra show the effects of boiling the film in H_2O for 30 min, and flash annealing.

Table III. SiO(s) and OH(s) Values, Before and After Heatings. ΔA is the Peak Amplitude, and INTG is the Area Integral of the Band.

	Just Deposited	5 Days	After D.I. Boil	After 9 Day Hold	After FA
SiO(s) Band	1056.5	1064	1068.5	1068	1063
SiO(s) FWHM	100	80.5	78.7	83.0	94.4
SiO(s) ΔA	0.2897	0.3034	0.3003	0.2728	0.2800
OH(s) Band	3650	3613	3634	3657	N/A
OH(s) INTG	4.3	8.36	6.50	9.18	0
OH(s) FWHM	370	425.3	416.2	499.5	0
OH(s) ΔA	0.0154	0.0186	0.0150	0.0158	0

mospheric H_2O with the formation of OH groups having a symmetric OH(s) ir absorption band (as well as a distinct band at 925 cm^{-1}) is on the order of days. The symmetric band on the other hand, leads us to conclude that for this slow process, there is an average spacing between interacting Si-OH groups, and a corresponding normal distribution of Si-OH groups about that mean value, (symmetric band). This is explored in greater detail below.

OH(s) Band Interpretation

By examining the initial asymmetric OH band, and understanding the local environments of Si-OH groups and the interactions between them, something can be learned about the distribution of these groups in the film. The vibrational modes of Si-OH groups are measurably affected by hydrogen-bonding interactions. Based on previously reported studies of SiOH and OH bands in a variety of organic materials, the structure of the OH(s) band, in particular the shift to lower wavenumber, derives from hydrogen bonding interactions between the positive space charge of the H atom of the OH group and negative space charge regions of the host material.[12] The negative space charge regions are associated with the non-bonding electrons of oxygen atoms in either Si-O-Si groups or Si-OH groups.[13] Specifically, the hydrogen bonding (H-bonding) interaction is between an H atom and another O atom not directly bonded to it, (represented by OH···O). Because the negative space charge region of the oxygen atom in Si-OH groups is greater than in Si-O-Si groups, the strongest of these interactions is between the OH pairs of neighboring Si-OH groups. The less negative space charge of Si-O-Si groups originates from the interaction of the non-bonding *p* electrons of the O atom with anti-bonding *d* states of the neighboring Si atoms.[13] It is found that as the O···O distance decreases, the H-bonding strength increases and the frequency of the O-H stretching vibration decreases.[14] Small changes in the O···O distance, *e.g.* changes of ~0.02Å can result in large shifts of ~50 cm^{-1} in the OH(s) frequency.[14] Therefore, the strong relationship between frequency and O···O distance, allows one to interpret differences in absorption frequency in terms of differences in spatial correlation between the interacting Si-OH groups.

The asymmetric broadening of the OH band derives from the existence of a continuous range of O···O distances, from nearly isolated Si-OH groups accounting for the absorption on the high frequency side of the absorption band, to closely associated Si-OH groups accounting for the low frequency absorption. This apparently random arrangement, suggests that there is no specific spatial relation between the interacting Si-OH groups. It is in this context that the Si-OH groups are spatially uncorrelated. In contrast, the symmetric feature with a spectral peak at about 3480 cm^{-1} that develops in films exposed to atmospheric H_2O, derives from spatially correlated, near-neighbor Si-OH groups having a *specific* average O···O separation, *i.e.*, from Si-OH groups forming a particular bonding configuration. This specific arrangement of atoms may also account for the occurrence of the 925 cm^{-1} SiOH band. We propose that such bonding configurations derive from the interaction between water molecules and the more reactive Si-O-Si bonds of the host SiO_2 network. As the Si-O-Si bond angle decreases, the Si-O-Si group becomes more reactive,[15] and the removal of these groups by water, converting them to near-neighbor Si-OH groups, is consistent with the shift of the SiO(s) spectral peak to higher wavenumbers as discussed in the following section.

We make one final comment concerning the formation of the asymmetric OH(s) band. Whereas interactions with atmospheric water vapor clearly lead to reaction pathways promoting near-neighbor Si-OH groups, the reactions occurring in the chamber after deposition appear to have a different origin which leads to uncorrelated Si-OH groups, *i.e.*, it is possible that the in-chamber incorporation mechamism is different. The mechanism may however involve molecular species, presumably containing OH groups that *derive in part* from the H_2O by-product of the deposition reactions that are carried out at high O_2 flow rates, We have noted that incorporation of OH groups is not accompanied by any spectral features related to the presence of SiH bonding groups, which would be readily detected by the bond stretching and bond bending bands at about 2265 and 875 cm^{-1}, respectively.[16] This would tend to rule out OH formation mechanisms based on molecular H_2; for if H_2 broke an Si-O bond of a Si-O-Si group, we might also expect SiH groups to form in addition to the Si-OH group.

SiO(s) Band Interpretation

The reason that the films discussed in the paper are particularly susceptible to post-deposition OH incorporation is that the material has a significant number of highly distorted Si-O-Si bonds which are more reactive than relaxed Si-O-Si bonds. For example, as shown in Fig. 4, the SiO(s) spectral peak of the first spectrum is at 1056 cm^{-1}, whereas the peak position of this band in thermally-grown and relaxed oxides is at 1078 cm^{-1}.[15] The position of the spectral peak can be correlated with the average bond-angle at the oxygen atoms sites (*i.e.*, the Si-O-Si angle). This angle is approximately 144° in relaxed thermal oxides, and is generally about 5–10° less in the Remote PECVD oxides. It is well-established that the reactivity of Si-O-Si groups is greater the smaller the bond angle at the oxygen site.[17] In addition, we have found that Remote PECVD oxide films are less dense than fully relaxed thermal oxides. This is examplified by higher etch rates in buffered HF, and by direct measurements of film thickness as a function of post-deposition thermal annealing.[18] This means that as-deposited films contains more reactive bonds, and has a porosity that allows for a rapid in-diffusion of small molecules.

The changes that take place in the spectral peak and width of the SiO(s) band with increasing OH incorporation substantiate this picture. Specifically, with increasing OH incorporation, the spectral peak shifts to higher wavenumber and the FWHM decreases. Both of these trends are in accord with removal of Si-O-Si bonds at the low wavenumber side of the distribution. This is further exemplified by a steepening of the low wavenumber side slope of the SiO(s) band. As these narrower angle bonds are removed, the distribution of absorbing SiO units in the film shifts to larger angle bonds, and the overall spread in the distribution diminishes (FWHM decreases). Moreover, the Remote PECVD SiO_2 films can be made immune to attack by atmospheric water by annealing for short-times (FA) at sufficiently high temperatures, >700–800° C (Fig. 7). Heating the oxide reverses the OH formation reaction, and provides enough molecular motion for most of the bonds to rearrange in a more relaxed state.[19] The temperature and time of the FA used in these experiments was insufficient to completely relax the Remote PECVD oxide, but it has been shown elsewhere that FA or rapid thermal annealing (RTA) at higher temperatures, >1050° C for 100s can render Remote PECVD oxides essentially indistinguishable from a thermally grown oxide processes at the same temperature.[19]

V. SUMMARY

We have shown that there are two sources from which Si-OH groups can form in oxide films deposited at low temperatures by Remote PECVD, both of these are via extrinsic processes: (i) OH species present in the chamber as a by-product of the deposition reactions; and (ii) H_2O present outside the chamber in the atmosphere. Atmospheric H_2O preferentially reacts with Si-O-Si groups with smaller bond angles. These bonds are more reactive than relaxed Si-O-Si bonds, and perhaps more accessible to attack because of localized increases in the bond-free volume that are evident in the increased etch rates of these films in buffered HF.[5] The molecular species and the reaction pathway for intra-chamber OH incorporation appears to be different than the atmospheric mechanism. At this time it is not possible to propose a specific OH containing species or a particular pathway that will lead to random, rather than spatially correlated Si-OH groups.

We have further shown that a-Si:H films (with about 5 at. % H, and 800Å thick) can act as diffusion barriers that serve to prevent OH incorporation in the chamber, and in the laboratory ambient. Flash annealing the films immediately after deposition not only relaxes the bond-angle distribution,[18] but also renders the film immune to attack by atmospheric water with two mechanisms contributing to the chemical inertness: (i) the relaxation of the Si-O-Si bond angle distribution to larger bond angles, and hence less reactive configurations; and (ii) film densification which limits the in diffusion of atmospheric H_2O, and also etchants such as buffered HF. Finally, we have shown, in this paper and in previous publications, that OH can be eliminated from SiO_2 thin films by an appropriate choice of deposition and post-deposition conditions, and that the incorporation of OH groups in the films discussed in this paper was intentional and not in any way an inherent characteristic of the Remote PECVD process.

ACKNOWLEDGMENTS

This work was performed under a grant from the NSF Engineering Research Center for Advanced Electronic Material Processing and under Office of Naval Research (ONR) contracts N00014-79-C-0133 and N00014-89-C-1507.

REFERENCES

1. D. W. Hess, J. Vac. Sci. Technol. *A2*, 244 (1984).
2. A. C. Adams. Solid State Technol. *26*, 135 (1983).
3. S. S. Kim, D. V. Tsu, G. Lucovsky, G. G. Fountain and R. J. Markunas, Mat. Res. Soc. Proc. *146*, 1989.
4. D. V. Tsu, G. N. Parsons and G. Lucovsky, J. Vac. Sci. Technol. *A7*, 1115 (1989).
5. D. V. Tsu and G. Lucovsky, Mat. Res. Soc. Proc. *131*, 289 (1988).
6. J. Batey and E. Tierney, J. Appl. Phys. *60*, 3136 (1986).
7. D. V. Tsu, and G. Lucovsky. Mat. Res. Soc. Symp. *77*, 595 (1987).
8. D. V. Tsu, G. Lucovsky, M. Mantini and S. S. Chao, J. Vac. Sci. Technol. *A5*, 1998 (1987).
9. G. N. Parsons, D. V. Tsu, C. Wang and G. Lucovsky, J. Vac. Sci. Technol. *A7*, 1124 (1989).
10. J. Theil and D. V. Tsu, unpublished data.

11. W. A. Pliskin, J. Vac. Sci. Technol. *14*, 1064 (1977).
12. W. C. Hamilton and J. A. Ibers, Hydrogen Bonding in Solids (W. A. Benjamin Inc., NY 1968) Ch. 3.
13. Helmut Knözinger, "Ch. 27: Hydrogen Bonds in Systems of Adsorbed Molecules", The Hydrogen Bond v III, Schuster, Zundel, and Sandorfy eds. North Holland Publishing Co., New York City, 1976, 1265.
14. A. Novak. *Structure and Bonding*. J. D. Dunitz, *et al.*, eds. *18*. Springer-Verlag, New York, 194 (1974).
15. R. L. Mozzi and B. E. Warren, J. Appl. Cryst. *2*, 164 (1969).
16. D. V. Tsu, B. N. Davidson, and G. Lucovsky, Phys. Rev. B. *41*, 1795 (1989).
17. M. D. Newton and G. V. Gibbs, Phys. Chem. Minerals *6*, 221 (1980).
18. J. T. Fitch, S. S. Kim, C. H. Bjorkman and G. Lucovsky, J. Electron. Mater. 157, *19* (1989).
19. E. A. Irene and E. Tierney, J. Electrochem. Soc. *129*, 2594 (1982).